# HIGH POWER SHARP PULSE MICROWAVE DISCHARGE: INTERPULSE REGIME

Sudeep Bhattacharjee and **Hiroshi Amemiya**

*Plasma Physics Laboratory, The Institute of Physical and Chemical Research (RIKEN), Hirosawa 2-1, Wako-shi, Saitama 351-0198, Japan*

*The Graduate School of Science and Engineering, Saitama University, Shimo-Okubo 255, Urawa-shi, Saitama 338-8570, Japan*

## 1. Introduction

High power short pulse microwave discharge is of current interest [eg. 1,2]. Our recent study has shown that the plasma state between the pulses (interpulse plasma) is also a useful phase of the discharge [3]. The high power during the pulse generates a strong electric field which raises the electron temperature $T_e$. The high $T_e$ favors ionization and assists plasma build up even during the interpulse regime. Thus an almost field free, energy sourceless but active plasma can be produced. Moreover, the choice of pulse width and the pulse repetition frequency could be important for plasma parameter control. Microwave plasma production in waveguides with a transverse dimension smaller than the cutoff value has an advantage of obtaining a high density narrow cross sectional plasma. Our studies using microwaves in the cw mode demonstrated that a plasma could not only be produced in the narrow waveguide but also the density could be higher than the cutoff value [4-6]. The present study relates to these possibilities in the case of pulsed microwaves. In what follows, we describe an experiment on the cutoff problems using short pulse high power microwaves. The plasma production and properties are discussed at a relatively higher pressure regime.

## 2. Experimental apparatus and method

Figure 1 shows a schematic of the experimental apparatus. Microwaves of 3 GHz with a power (60-100 kW) produced by a magnetron PM were pulse modulated with a short pulse (0.05 - 1.0 μs) and a repetition frequency of 10 - 500 Hz. The waves were guided through a coaxial cable CX, a power monitor PM, a matching M, a rectangular bend H and a quartz window W into a circular waveguide CW (37 cm in length, 5.74 cm ϕ) located inside a vacuum chamber C. The diameter of CW is slightly less than the cutoff value. CW was inserted into a multicusp MC constructed with permanent magnets to provide a minimum-B field for particle confinement. A trigger signal Trig was used for pulse initiation and a reference signal for diagnostics. PC is a computer for storing data. The current decay profiles and probe characteristics were measured by a Langmuir probe P (plane, 5 mm ϕ) using a digital oscilloscope DSO with time averaging (64 shots) and a Boxcar integrator BX. For measuring the decay profiles of ion ($I_+$) and electron currents ($I_e$) the probe was biased at -70 V and 20 V respectively. For obtaining the probe characteristics using the Boxcar, the gate aperture was set at 0.1 μs and the decay to 30-50 μs was measured in steps of ~ 1 μs by a slow scanning of the probe voltage. From the probe characteristics the temporal variation of $T_e$ and $N_e$ were deduced. The electric field E was measured using a needle type probe with a 1.5 mm length aligned parallel to the electric field in the circular mode. The electric field impulse was

rectified by a diode responsive to the GHz range microwave field. The axial variations of $I_+$ and E were measured in DSO by moving the respective probes along the waveguide and recording the peak current and the field signal.

### 3. Experimental results

Figure 2 shows typical spacio-temporal profiles of $I_+$ at a pressure p = 2.0 Torr with the axial distance along the waveguide z (cm) as a parameter. z = 0 corresponds to the entrance of the waveguide at the microwave input side. Time t=0 corresponds to the beginning of the pulse whose width $t_w$ is ~1 μs. The plasma is produced inside the narrow waveguide. It should be noted that the peak current spatially falls along the waveguide, but rises after z = 18 cm to a second maximum around 26 cm and finally falls beyond 30 cm. Thus two regions with higher plasma density have been identified, the peak current of the latter being usually ~ 50 % of the first.

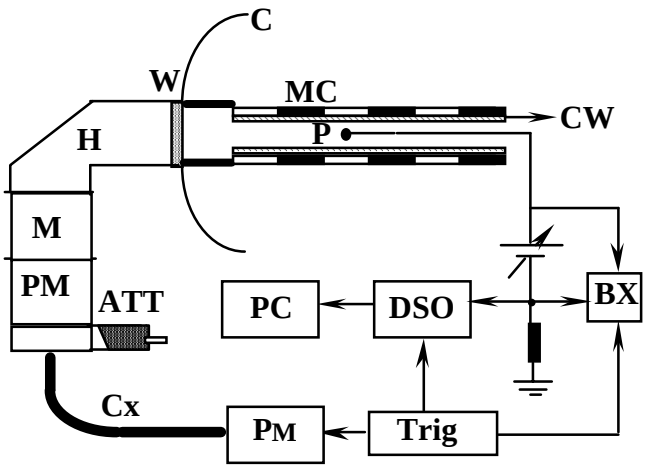


**Fig. 1.** Schematic of the apparatus.

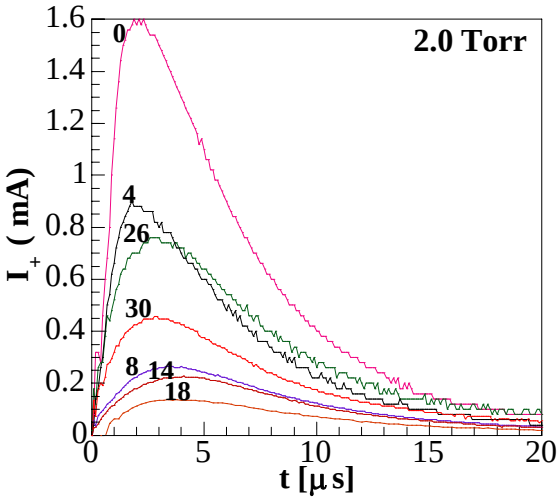


**Fig. 2.** Ion current profiles.

Figure 3 shows the form of $I_e$ build up and decay at z = 2 cm for different p. It is clearly seen that the build up occurs even after the end of the pulse, 2-15 μs. The build up is faster at a higher p. At locations farther away from the entrance eg. Z = 10-15 cm, the build up was delayed at a higher p. However, again at $z = z_m$ = 20-30 cm (region of second current peak in Fig. 2), the build up followed that of z = 2 cm. Therefore, the build up process could be different between the two regions with a higher plasma density. The same feature has been found also for the ion current $I_+$.

Figure 4 shows the temporal variation of $T_e$ in the interpulse regime at z = 20 cm. $T_e$ shows a value of about 6-10 eV and is slightly higher just after the end of the pulse. $T_e$ depends weakly on p and the decay time scales are much longer than particle decay times. The effect of varying the pulse repetition frequency $f_r$ (10-500 Hz) and the pulse width $t_w$ (0.08-1.2 μs) on the peak currrent $I_m$ and the decay time constant τ was studied at z = 4 cm. An increase in $t_w$ leads to an increase in $I_m$ and τ, probably due to a greater energy input to the plasma. However, $I_m$ and τ weakly depended on $f_r$. This suggests that any charge accumulation by pulse repetition was small.

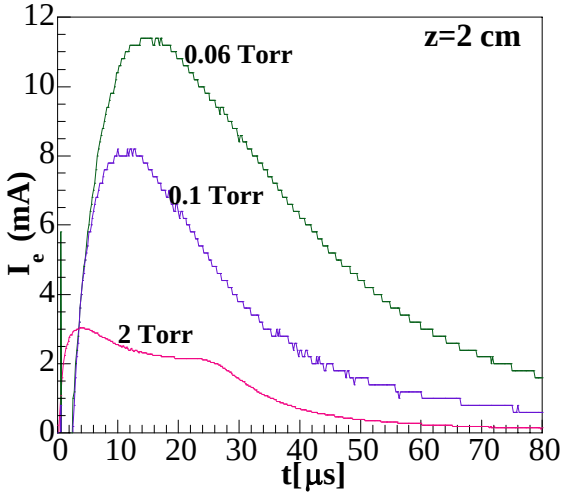


**Fig. 3.** Electron current build up.

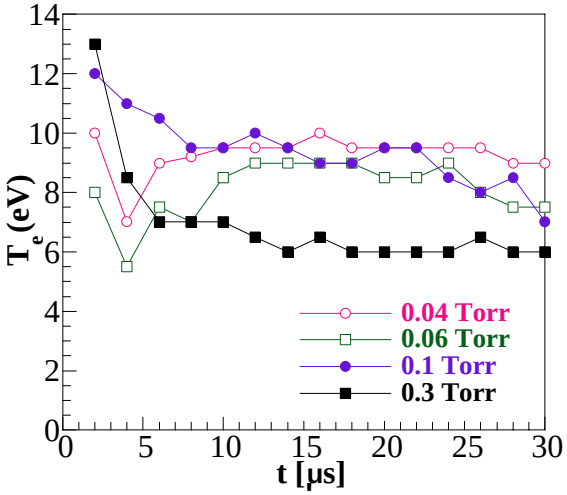


**Fig. 4.** Variation of the electron temperature.

Figure 5 shows the axial variation of the ion density $N_+$ along the waveguide at different p measured at t = 10 μs. Plasma density indicated a value over $10^{10}$ $cm^{-3}$. It is seen that $N_+$ is peaked near z = 0 cm and a second peak appears at $z_m$ = 20-30 cm. Between the two regions $N_+$ decreases to a smaller value (z=10-15 cm). Although $N_+$ at z = 7-20 cm appears to be very small in the linear scale, the actual value lies in the range of $10^9$ $cm^{-3}$ when plotted in the semi-log scale.

Figure 6 shows the axial variation of the electric field E at the same p as in Fig. 5. The variation of E closely resembles that of $N_+$ in Fig. 5, suggesting a correlation between E and $N_+$. The values of E at z = 7-20 cm appears to be very small but they are actually finite.

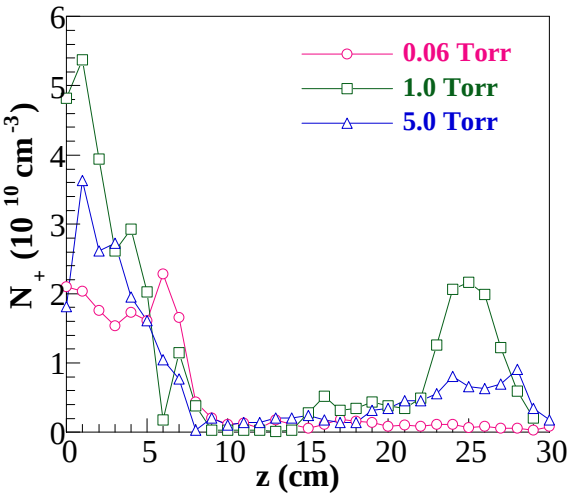


**Fig. 5.** Axial variation of the ion density.

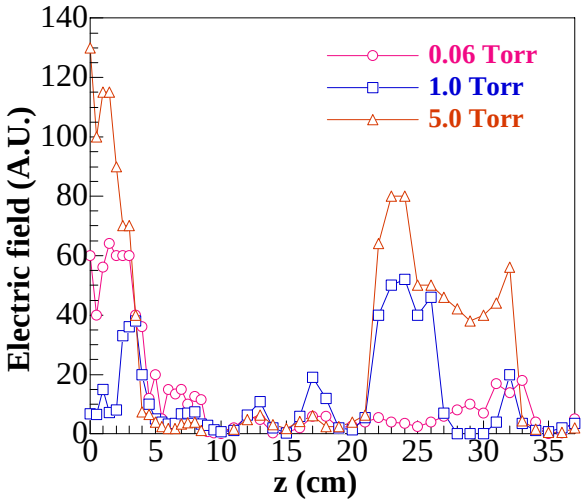


**FIG. 6.** Axial variation of the electric field.

## 4. Discussion

The quicker build up with pressure of $I_e$ (Fig. 3) at z~0 and $z_m$ can be explained by the higher ionization efficiency with p since the electric field was stronger at these positions (Fig. 6) while the slower build up with pressure at the intermediate region (z=10-15 cm) can be due to the diffusion. The coincidence between the axial variations of $N_+$ and E (Figs. 5 and 6) supports this view. Similar interpretation can be made for the build up of $I_+$. The facts that $I_+$

and $I_e$ continue to build up after the end of the microwave pulse (Figs. 2 and 3) can be due to the continuation of high $T_e$ (Fig. 4). This helps to maintain the interpulse plasma. Although two peaks were observed in the axial density distribution, the distribution became more uniform at a lower p. However, the result at higher p helped us to investigate the mechanisms of plasma production in the narrow waveguide.

The production of plasma in the narrow waveguide may be described by the ionization due to the penetrating E and the high $T_e$ as well as the diffusion. The field E near the entrance creates a dense plasma, which diffuses. A convex shape of the plasma at the entrance diverges the wave which would be reflected by the wall and converged in the second region ($z=z_m$). The temporal behavior and the axial variation of N+ are considered to be governed by the particle balance equation, obtained by assuming the diffusion model at a higher p:

$$\frac{\partial N_+}{\partial t} + v_z \frac{\partial N_+}{\partial z} - D\frac{\partial^2 N_+}{\partial z^2} - D_r \frac{1}{r}\frac{\partial}{\partial r}\left( r\frac{\partial N_+}{\partial r}\right) + \beta N_+ = 0 \quad , \tag{1}$$

where $\beta$ is the decay constant given by the radial diffusion and ionization ($\beta=(c/R)^2 D_r - \alpha$, $\alpha$: ionization rate, R: waveguide radius, c: constant, 2.4 for Bessel-type distribution), D and $D_r$ are longitudinal and radial diffusion coefficients respectively and $v_z$ is due to a driving force by E which would be mainly felt by the electrons. The solution would be:

$$N_+(z,t) = \frac{2}{\sqrt{\pi}} \sum_i N_i \int_{z_i}^{\Delta z} \int_0^{t_w} \frac{\exp\{-\beta(t+t')\}}{\sqrt{4D(t+t')}} \exp\{-\frac{(z - z_i + z - v_i(t+t'))^2}{4D(t+t')}\} dt'\, dz' \quad , \tag{2}$$

where $z_i$=position at z~0, $z_m$ (corresponding to the positions of two peaks in N+), $\Delta z$ is the initial plasma width, $N_i$ and $v_i$ are the initial plasma density and a driving force by E at $z_i$. If the waveguide has a diameter above the cutoff value the wave propagates freely into it, then we may put $\Delta z \rightarrow \infty$ in Eq. (2) and the spatial integration becomes unity and drops out. The temporal integral reduces to $N+ \sim \exp(-\beta t)$, which was previously obtained for the case of a recombination free decay [3].

## 5. Conclusion

It has been shown that pulsed microwaves can produce a plasma in a narrow tube with a cross section smaller than the cutoff value. The mechanism of creating the interpulse plasma has been found to be due to the penetration of electric field, the high electron temperature after the pulse and the charged particle transport. Although the above experimental results are concerned with higher pressures, the plasma unifomity increases at a lower pressure. The results may be useful for certain applications requiring a plasma in a narrow cross section.


[1] C. A. Sullivan, W. W. Destler, J. Rodgers, and Z. Segalov, J. Appl. Phys. **63** 5228 (1988).

[2] G. A. Askaryan, G. M. Batanov, A. E. Barkhudarov, S. I. Gritsinin, E. C. Korchagina, I. A. Kossyi, V. P. Silakov and N. M. Tarasova, J. Phys. D: Appl. Phys., **27** 1311 (1994).

[3] S. Bhattacharjee and H. Amemiya, J. Appl. Phys. **84** (1998) *in press.*

[4] H. Amemiya and M. Maeda, Rev. Sci. Instrum. **67** 769 (1996).

[5] S. Bhattacharjee and H. Amemiya, *Proc. 3rd International conf. on reactive plasmas,* Nara Japan, pp. 407-408 (1997).

[6] S. Bhattacharjee and H. Amemiya, Rev. Sci. Instrum. **68** 3061 (1997).